WHAT EXACTLY DOES THE NOSE KNOW? A CHARACTERIZATION OF AVERSIVE STIMULUS-EVOKED ACTIVITY IN THE EARLY OLFACTORY CIRCUIT

By

KEITH A. PERKINS JR.

A thesis submitted to the

School of Graduate Studies

Rutgers, the State University of New Jersey

In partial fulfillment of requirements

For the degree of

Master of Science

Graduate Program in Psychology

Written under the direction of

John P. McGann

and approved by

_____

_____

_____

New Brunswick, New Jersey

January, 2020

ABSTRACT OF THE THESIS

WHAT EXACTLY DOES THE NOSE KNOW? A CHARACTERIZATION OF AVERSIVE STIMULUS-EVOKED ACTIVITY IN THE EARLY OLFACTORY CIRCUIT

By KEITH A. PERKINS JR.

Thesis Director:
John P. McGann

The ability to learn from previous experiences and use them in current circumstances is a skill that is necessary for success in any environment. This skill is dependent on our ability to learn, which requires an understanding of the relationships between encountered stimuli. Accumulating evidence shows that learning the relationship between stimuli can occur even in early sensory processing regions in the brain, even in places that seemingly lack of knowledge about stimuli occurring in other sensory modalities. To test what information an extremely early sensory region might have about other stimuli (or their outcomes for the organism), we used optical neurophysiological methods to observe neural activity in the mouse olfactory bulb during the presentation of aversive electrical stimulation of the tail. The results demonstrated that populations of PG, SA, and M/T neurons in the olfactory bulb respond not only to odors but also to tailshock. These responses are not directly evoked by peripheral input from OSNs, which did not exhibit any response to shock. Nonetheless, the response to shock in these neuronal populations

were eliminated when the peripheral airflow was shunted away from the nose by a tracheotomy or when the ipsilateral airflow was prevented via naris occlusion. Pilot data demonstrated that various types of aversive stimuli besides tailshock evoked similar patterns of bulbar activity. These data demonstrate that during odor-cued fear learning, which is known to induce local, stimulus-specific plasticity in these populations of neurons in the olfactory bulb, information about an olfactory conditioned stimulus (CS) converges with activity driven by a somatosensory unconditioned stimulus (US) as early as the olfactory bulb glomeruli. This could underlie sensory changes associated with associative learning.

Acknowledgements

I would like to thank the members of my thesis committee, Dr. Kasia Bieszczad and Dr. Benjamin Samuels. I also want to thank my advisor, Dr. John P. McGann for his help and guidance.

Table of Contents

List of Tables

Introduction

Humans are constantly changing organisms living in a constantly changing environment. To survive, our brains must adapt to integrate the current state of the outside world[1]with our own current motives and needs. The heart of this flexibility is learning. Learning enables a naïve organism to choose behaviors that lead to desired outcomes and avoid negative consequences. These choices require the organism to anticipate the future based on the current state of the world and the memory of what's happened in the past. To do so effectively, an organism must understand the conditional relationships among external stimuli and between stimuli and future outcomes.

Learning that the occurrence of one stimulus is conditioned on the occurrence of another is called associative learning. For such learning to happen, information about both stimuli must converge someplace in the brain at the same place and time (even if the stimuli themselves are not simultaneous). Ascertaining the neural locus of such convergence and the biological mechanisms that link stimulus representations together has been the focus of a century of work [2-10]. For instance, one of the now classic lines of research observed that in auditory fear conditioning, where a tone predicts an aversive footshock, information about the tone and the shock converges in the amygdala [8], where co-occurrence of neural activity can induce synaptic plasticity . Different stimuli (e.g. pure tone vs complex sound) and different paradigms (e.g. temporally overlapping stimuli vs stimuli with a time-lag between them) engage different brain regions [11] but ultimately still require convergence of information about the stimuli someplace in the brain.

Because associative learning readily encompasses stimuli from different sensory modalities, these areas of convergence have historically been presumed to be polymodal, "higher level" brain structures. However, a growing body of evidence shows that even early sensory processing regions somehow undergo plasticity after associative learning, despite the seeming lack of information about stimuli of other modalities. Such changes have been shown in primary sensory cortices[12-22], sub-cortical sensory structures [23-27], and even primary sensory neurons [28, 29]. It remains unclear how these seemingly unimodal sensory regions "know" about stimuli outside their own modality.

What is the purpose of sensory plasticity following learning? Depending on the circumstances of the initial learning, the corresponding neural changes may serve to enhance the sensory processing of important stimuli. For instance, the primary auditory cortex can rapidly change to emphasize the amplitude, frequency, or azimuth of a sound depending on which of these stimulus features predict an ecologically-important outcome[22, 25, 30]. Even different learning strategies within a given behavioral task can result in corresponding forms of sensory plasticity [31, 32]. However, stimulus-specific associative plasticity occurs even when sensory stimuli are unambiguous, suggesting that mere improvement in sensory function may not be its primary function. Instead, this plasticity may serve to regulate attentional focus, balance the systemic metabolic load, and most importantly for our purposes facilitate neuroplasticity. [18].

These findings illustrate the interplay between peripheral input from the environment and previously learned information about the meaning or importance of incoming stimuli. This is mirrored by the circuit level anatomy of the brain where "ascending" input reflecting current sensory input is shaped by "top-down" influences,

including “descending” projections from higher brain regions, endocrine factors [33], and neuromodulators [22, 34-36]. In many sensory systems these “top-down” connections substantially outnumber the ascending ones [36, 37]. The existence of such early, unimodal sensory processing regions presents the possibility that such structures are not strictly unimodal at all.

In the olfactory system, the first convergence of ascending sensory signals with “top-down” centrally originating signals occurs in the brain’s olfactory bulb. This structure is uniquely experimentally accessible via a combination of transgenic mice and optical neurophysiological approaches that permit direct observation of activity in specific cell populations, including the axon terminals entering the brain from the nose, in a living, breathing, smelling animal. In previous work, we and others have observed multiple forms of learning-related plasticity throughout the circuit [28, 29, 38], but it remains unclear how the bulb knows about cross-modal contingencies.

One advantage of the olfactory circuit is that the chemical identity of each odor is mapped onto space in the olfactory bulb. The olfactory sensory neurons (OSNs) in the nose express one out of a thousand odor receptors on their cilia which lie in the olfactory epithelium (OE). They send their axons through the cribriform plate into the olfactory bulb where they organize themselves into distinct neuropils called glomeruli.[39, 40]. Depending on the chemical structure of the odorant it binds to different odor receptors, exciting the OSNs expressing those receptors, and thus driving neurotransmitter release from the OSN terminals in specific glomeruli in the olfactory bulb. Within the glomerulus, OSNs synapse onto the dendrites of mitral cells, the principal output neurons of the olfactory bulb, which send axons to many brain regions including the piriform

cortex, anterior olfactory nucleus, amygdala, entorhinal cortex, and hypothalamus. Each glomerulus is ringed by periglomerular (PG) cells, GABAergic interneurons and by joint dopamine/GABA-releasing neurons called short axon (SA) cells that interconnect across glomeruli. All three types of cells are driven by OSN activity but also influenced by serotonergic, noradrenergic, and cholinergic neuromodulatory inputs and by "top-down" projections from olfactory cortices[36], hippocampus, and basolateral amygdala. By selectively expressing fluorescent activity indicators in each of these cell types, we are able to observe neural activity at each stage of the circuit [41].

In previous work, we have demonstrated that olfactory fear conditioning evokes plasticity in various parts of the olfactory bulb circuit. Discriminative fear conditioning, where the mouse is trained to be afraid of one specific odor that predicts an aversive footshock, evokes dramatic increases in OSN synaptic output evoked by the conditioned odor but not control odors [28]. Generalizing fear conditioning, where the mouse is trained to be afraid of an odor but actually becomes afraid of many odors evokes big increases in odor-evoked activity in the PG cells [42], perhaps reflecting corresponding increases in the OSN output (Rosenthal et al. In Progress). These changes can occur within a day of learning and can persist for months [32]. Similar findings have been reported by others in the mitral cells [38]. However, it has been a mystery how these olfactory bulb neurons could "know" about the footshock. Associative learning has always been understood to require convergence of information about the associated stimuli, so this gap in our knowledge could prove essential to understanding how the brain learns relationships among stimuli in the environment. Which could give us A mechanism that explains why individuals who experience traumatic events become hypersensitive and/or hypervigilant.

Materials and Methods

Animals

In these experiments 23 experimentally naïve adult mice between the ages of 3 to 11 months were used. The mice were single housed in open top shoebox cages with food and water provided ad libitum. These mice were also kept on a 12hr light/dark cycle. All procedures described herein were approved by the Rutgers University Animal Care and Use Committee.

Animal Lines

PG Cells

In order to view the activity of the periglomerular interneurons (PG cells) one set of mice (n=7) resulted from a cross between mice from the GAD2-IRES-Cre driver line (stock#: 010802, The Jackson Laboratory) that bicistronically expresses cre recombinase from the promoter for gad2, the gene that encodes glutamic acid decarboxylase 65(GAD 65; 42), with mice from the Ai95 reporter line (stock #024105, The Jackson Laboratory) that include the calcium indicator GCaMP6f sequence under control of the endogenous Gt(ROSA)26Sor promoter/enhancer regions and the CAG hybrid promoter but with a floxed STOP codon. This results in the expression of GCaMP6f in GAD65-expressing cells throughout the brain [41, 43]. There was also a second group of mice (n=4) that resulted from GAD2-IRES-Cre recombinase mice (stock#010802, The Jackson Laboratory) , in which GCaMP6f expression was induced via an intrabulbar injection of a viral vector (AAV9) carrying a floxed-STOP gene for GCaMP6f three to five weeks before imaging. In both groups the result was an animal that expressed GCaMP6f in all GAD65-expressing cells in the olfactory bulb as previously reported.

Short Axons Cells

In order to view the activity of the dopaminergic (andGABAergic) Short Axon cells (SACs) one set of mice (n=5) mouse resulted from a cross between the (DATIREScre) driver line (stock#: 006660, The Jackson Laboratory) that expresses cre recombinase from the promoter for the gene SLC6A3, the gene that encodes Dopamine Transporter (DAT) [44], with mice from the Ai95 reporter line (stock #024105, The Jackson Laboratory) that include the calcium indicator GCaMP6f sequence under control of the endogenous Gt(ROSA)26sor promoter/enhancer regions and the CAG hybrid promoter but with a floxed STOP codon. This results in the expression of GCaMP6f in all DAT-expressing cells throughout the brain.

Mitral Cells

One set of mice (n=8)resulted from a cross between the Tbet-cre driver line (stock#: 024507, The Jackson Laboratory) where cre recombinase expression is driven by the Tbox21 promoter (so cre is expressed in all cells that produce the T-box transcription factor) 44 , with mice from the Ai95 reporter line (stock #024105, The Jackson Laboratory) that include the calcium indicator GCaMP6f sequence under control of the endogenous Gt(ROSA)26S or promoter/enhancer regions and the CAG hybrid promoter but with a floxed STOP codon, resulting in the expression of GCaMP6f in all Tbx21 -expressing cells (Mitral Cells) which is specific to the mitral cell layer in both the main and accessory olfactory bulbs. [45]

Olfactory Sensory Neurons

Finally the final set of mice (n=3) resulted from a cross between the OMP-cre driver line (JAX stock #006668,The Jackson Laboratory), which expresses olfactory marker protein (OMP) in all mature OSNs, with mice from the Ai95 reporter line (stock #024105, The Jackson Laboratory) as above. In this driver line, the gene for cre recombinase replaces the coding region of the gene encoding OMP, so experimental animals are heterozygous for both OMP and GCaMP6f.

In vivo Optical Imaging

Apparatus

The imaging protocol was used as previously reported in [1, 28, 34, 46]in order to view the activity of each cell population in vivo we used fluorescence epillumination on a custom Olympus BX51 microscope with a 4X (0.28 NA) objective. Illumination originated from a bright LED (470nm wavelength, Thorlabs, Newton,NJ). The neuronal activity of each cell population was captured with a back-illuminated, monochrome CCD camera (NeuroCCD, SM-256, RedShirtImaging, Decatur, GA) at a pixel resolution of 256x256. All imaging data was collected with a frame rate of 50 Hz and a total trial time of 20 seconds unless noted. Data collection and camera controls was done by using Turbo-SM™.

Respiration and Heart Rate Measurement

Respiration was measured by using a piezoelectric strip placed on the chest wall to measure chest expansion. The signal from the piezo was amplified by using a CWE BMA-931 AC/DC Bio amplifier. Heart rate was measure using a CT-1000 Cardiotachometer. Electrodes were placed on both forepaws and the right hind paw.

Odor Trials

Methyl valerate at 99% purity (Sigma-Aldrich, St. Louis, MO) was presented using a custom 8-channel vapor dilution olfactometer. Methyl valerate was diluted to a desired concentration in clean air using nitrogen as a carrier gas. Each odor trial consisted of a 4s pre-odor period followed by a 6-sec odor presentation period and a subsequent 10 sec post odor period.

Noxious Stimulation

The shocks were delivered from a Grass Instruments stimulator set to deliver a voltage of 50V at a rate 200 shocks/s for 200ms totaling 40 stimulations per trial. The electrodes attached to the tail were made of a metal plate screwed into a small lightweight Teflon block and the entire electrode was covered with non-conductive tape to ensure no loss of power due to inadvertent contact with the metal mouse holder. The ITI for each shock trial was a minimum of 1 min (unless otherwise noted). All aversive stimulation trials consisted of a 10 s pre-shock period followed by the 200ms shock train and a subsequent 9.8 sec post shock period. For thermal stimulation, the left hind paw was contacted momentarily with a cautery tool. For indirect trigeminal nasal stimulation, lab grade pure CO2 was presented at various dilutions in clean air for 6 sec. CO2 sometimes induced changes in breathing rate, necessitating a longer ITI to allow the breathing rate to return to baseline.

Surgifoam Experiments

In one mouse from each cell type except the OSN mice were tested using this paragigm. The imaging began with a baseline block of 2 trials of Methyl Valerate presentation, 10 Blank trials, and 10 Shock trials. The surgifoam was then implanted in the left nare and the experimental block began which consisted of 1-2 odor trials, 5 shock trials, and 5 Blank trials. Next, for the Post-surgi block the plug was removed from the left nare and 2 odor, 5shock, 5 blank trials were taken. Then A new piece of surgifoam

was used to block the opposite nare and the experimental block was repeated. The surgifoam was once again removed and the Post-surgi block was repeated.

Surgical Methods

Each mouse was first anesthetized with an intraperitoneal injection of pentobarbital and subsequent subcutaneous injections of 0.1% Atropine (to prevent excessive mucous secretion), 0.25% bupivacaine (as local anesthetic on scalp before scalpectomy and throat before tracheotomy), and 2mg/mL DexaJect™(to suppress inflammatory response after tracheotomy). Breathing was measured by a piezo sensor positioned to indicate expansion of the chest wall, providing us with the second derivative of intranasal airflow3. A scalpectomy was performed exposing the underlying skull and the periosteal membrane was scraped away and the skull dried with 70% ethanol. Mice were then secured to the custom head holder using Loctite™ superglue and dental acrylic. Once the mouse was secure a dental drill was used to make a bilateral thinned bone cranial window over the olfactory bulbs and topped with a coverslip as previously reported [28, 34, 46]

Data Analysis

The imaging data were analyzed as previously reported [28]. Briefly, the raw optical data was spatially median filtered to reduce shot noise, then low-pass temporally filtered at the Nyquist frequency to prevent aliasing. The regions of interest used to extract fluorescence traces were distinct focal glomeruli or the entire dorsal surface of the olfactory bulb. The data were analyzed using custom software in Matlab and Origin Pro.

Results

Response of Olfactory Bulb Neurons to Aversive Stimuli

The previous findings that OSN terminals, PG cells, and mitral cells can all exhibit associative plasticity after odor→tailshock fear conditioning suggested the hypothesis that neural activity evoked by the tailshocks could be converging with odor-evoked activity in the olfactory bulb. To test this hypothesis, we performed optical imaging of neural activity in the mouse olfactory bulb during the presentation of odors or tailshock. Note that this hypothesis specifies that the convergence occurs before any learning has taken place, so the following experiments are all performed in experimentally naive mice. The strongest test of this hypothesis would be to observe shock-evoked activity in the olfactory bulbs of anesthetized mice (so long as they still feel the shock), which would be consistent with a strong, hardwired circuit distributing shock information to other modalities.

We began by looking at the PG cells because they are known to exhibit associative plasticity after odor-cued fear conditioning [42], receive strong, amygdala-modulated neuromodulatory projections from locus coeruleus [34], and are richly innervated by descending projections from the olfactory cortices[47, 48]. We performed wide-field fluorescence imaging in a line of gene-targeted mice that express the fluorescent calcium indicator GCaMP6f under the control of the GAD65 promoter (PG-GCaMP mice), thus resulting in widespread expression of GCaMP in PG cells throughout the dorsal olfactory bulb. To capture the overall spatial extent of odor- and shock-evoked activity in these mice, we used a low magnification objective allowing us to simultaneously observe the entire dorsal olfactory bulb bilaterally.

As previously reported, odor presentation in these mice evokes strong respiration-coupled increases in fluorescence in an odor-specific subset of glomeruli (Fig. 1), typically 5-9% ΔF/F. Remarkably, the delivery of a 200 msec electrical stimulation of the tail also caused a stimulus-locked response in glomeruli throughout the dorsal olfactory bulb (Fig. 1), typically 2-3% ΔF/F. This response was always timed to peak during the inhalation phase of the respiratory cycle, sometimes persisting over multiple inhalations, and usually though not always beginning on the first cycle after stimulation (Fig. 3). Unlike odor-evoked PG cell activity, which always occurs as a set of discrete foci reflecting the subset of glomeruli receiving peripheral input from the nose, shock-evoked PG cell activity usually started in a discrete subset of glomeruli on the first inhalation (Fig. 3), but rapidly evolved to include many or most glomeruli throughout the dorsal olfactory bulb on one or two subsequent inhalations (Fig. 3A). The pattern of glomeruli activated during the initial responses did not obviously correspond to any particular odor (recall that these mice have not been fear conditioned or otherwise manipulated), and the later responses were distributed across many more glomeruli than are typically activated by any one odorant. This general pattern was highly reliable across five individual mice.

In the olfactory bulb, PG cells typically innervate only one glomerulus. By contrast, SA cells interconnect many different glomeruli. Given sequential spread of the shock-evoked activity from a few glomeruli to many glomeruli, we next imaged shock-evoked activity in a different line of mice expressing GCaMP6f under the control of the DAT promoter (SA-GCaMP mice) to visualize activity in these dopaminergic SA cells. In these mice, odor presentation evokes focal fluorescence signals in modest numbers of individual glomeruli, just like PG cells. When we presented tailshock stimulation, we

observed a pattern similar to that in PG cells, with a respiration-coupled response peak that evolved from a small number of glomeruli to much of the dorsal bulb across respirations (Fig. 3A). The responses were robust and unambiguous, but also substantially smaller than those evoked by odorant presentation (Fig. 1C). This pattern was highly reliable across five individual mice.

Given the strong tailshock-evoked activity of the PG and SA cells, we then tested the mitral/tufted cells, which compose the primary output of the olfactory bulb and also exhibit strong fear learning-induced plasticity [38]. If these cells respond to electrical stimulation of the tail, it would mean that the OB is not only receiving tailshock-evoked activity but also propagating that signal throughout the brain [49]. M/T cell activity was visualized in mice expressing GCaMP6f under the control of the Tbx-21 promoter (Mitral-GCaMP mice). The patterns of activity in these mice are normally more diffuse than the others, even with olfactory stimuli, because the depth of these cells and their lateral dendrites may produce a more scattered signal (Fig. 1D). Following shock presentation, the M/T cell populations responded strongly (typically 3-8% $\Delta F/F$) and broadly throughout the bulb on subsequent inhalations, as in the other cell types. Despite the initial breadth of the response, there was nonetheless a notable increase in the spatial distribution of activity across the second and sometimes third inhalation after the shock. This pattern held up across seven individual mice.

The final test was whether tailshock-evoked activity could be detected in the OSN terminals. Shock typically evoked a rapid inhalation, which could potentially have provided a strong peripheral drive into the bulb, thus stimulating other cell types without needing centrifugal input from elsewhere in the brain. To test this, we imaged from a line

of mice expressing GCaMP6f under the control of the OMP promoter, thus labeling all mature OSNs. In these mice, olfactory stimuli evoke the classic spatiotemporal pattern of inhalation-locked inputs to a modest number of discrete, odor-specific glomeruli. However, unlike the other cell types, tailshock evoked little or no activity in the OSNs (Fig. 1A) on any trial in any of three individual mice (despite robust olfactory-evoked responses in each). This suggests that the signal underlying the olfactory bulb response to shock is not mediated through the peripheral sensory input. (Fig. 5)

Role of Peripheral Signaling

Activity in the olfactory bulb has long been known to be coupled to the respiratory cycle [50], including spontaneous action potential firing, odor-evoked firing, and now tailshock evoked firing. It remains unclear whether this oscillatory activity is driven by airflow-evoked peripheral input, by centrifugal signals to the bulb from respiratory regions, or by a combination of the two. We tested the necessity of peripheral airflow by tracheotomizing mice so that they breathe through a tracheal tube with no airflow through the nose. If peripheral airflow played no role in the timing of shock-evoked bulbar activity we would expect to see continued responses to shock, possibly still in phase with the respiratory cycle (based on centrifugal inputs). Conversely, if tailshock only evoked measurable activity in the olfactory bulb circuit during inhalations because it required simultaneous peripheral input during shock-evoked centrifugal input, we would expect to see tailshock responses vanish after tracheotomy. As shown in Fig. 4, tracheotomy entirely eliminated tailshock-evoked responses in the olfactory bulb regardless of whether we looked at PG cells, SA cells, and M/T cells. To follow up on this finding we exploited the lateralization of the early olfactory system, where each bulb receives ascending input

only from the ipsilateral nasal cavity, to test the effects of unilateral elimination of peripheral airflow would impact tailshock-evoked activity. In one mouse or each strain (PG-GCaMP, SA-GCaMP, and M/T-GCaMP), we observed that reversible blockade of one naris with wet surgifoam entirely eliminated tailshock-evoked activity in the olfactory bulb ipsilateral to the blockade, an effect that reversed when the surgifoam was removed (Fig. 6).

Alternative Aversive Stimuli

The finding that tailshock evokes broad activity in the OB, even in anesthetized mice, raised the question of what range of aversive stimuli could evoke such a response and what information about those stimuli is actually represented in bulbar activity. As a pilot experiment to explore this question, we used one PG-GCaMP mouse where we presented multiple types of aversive somatosensory stimuli, including tailshock, thermal stimulation of the hind paw, and presentation of CO_2 to the nose (which evokes an uncomfortable “burning” feeling via trigeminal stimulation without any odor). Each of these stimuli evoked a physiological response, such as increased heart rate and respiration, despite the anesthesia. Interestingly, all three stimuli evoked broad, inhalation-locked activity across the olfactory bulb, though they differed in response amplitudes (Fig. 7). This demonstrated that the response in the bulb is not an artifact of electrical stimulation. Moreover, the spatiotemporal response patterns were extremely similar across stimuli, suggesting that at least at this coarse level of analysis they represent a shared state of aversion or arousal rather than specific information about the somatosensory stimulus itself.

Discussion

This study demonstrated that populations of PG, SA, and M/T neurons in the olfactory bulb respond not only to odors but also to aversive tailshock. These responses are not directly evoked by peripheral input from OSNs, which did not exhibit any response to shock. Nonetheless, the response to shock in these neuronal populations were eliminated when the peripheral airflow was shunted away from the nose by a tracheotomy or when the ipsilateral airflow was prevented via naris occlusion. Pilot data demonstrated that various types of aversive stimuli besides tailshock evoked similar patterns of bulbar activity.

The central finding of this study is that activity driven by odors and by aversive non-olfactory stimuli converge in the mouse olfactory bulb. This could permit local associative plasticity in the bulb during odor-cued fear conditioning. Previous studies have shown that such plasticity does in fact occur, but the mechanism by which the early olfactory system received this information (e.g. was the learning taking place elsewhere and then "downloaded" to the putatively unimodal olfactory bulb) has been elusive [18]. These findings support the possibility of direct learning of the CS-US contingency in the olfactory system itself and thus imply that such learned stimulus relationships may be distributed throughout the brain rather than being focused in a small number of specialized emotional learning centers [3, 8, 51].

The preliminary finding that various aversive stimuli evoked at least superficially similar patterns of activity in the olfactory bulb suggests that the information reaching the bulb may be limited. For instance, it likely does not know that the US was "a 200 msec stimulation of the tail" as opposed to knowing that "something bad happened" or perhaps

"something surprising happened" [52]or even as limited as "something happened." This is consistent with the known centrifugal innervation of the olfactory bulb, which includes prominent neuromodulatory inputs from structures like the locus coeruleus, raphe, and diagonal band of Broca [36, 53], but not extensive projections from other sensory regions. Some of this neuromodulatory input depends in turn on the output of classically fear-related amygdala subnuclei[34], suggesting a testable circuit-level model of how this information reaches the olfactory bulb. Further behavioral experiments, including the selective labeling of olfactory bulb "engram cells" with channelrhodpsin [10], may help to clarify the content of the memory encoded in the bulb.

OSNs do exhibit plasticity when odor is paired with shock (though not when shock is presented alone) [28], but we did not observe a direct response of OSNs to shock. A classically Hebbian model of CS-evoked and US-evoked activity convergence in the OSNs would be undermined by this finding. However, OSN terminals are strongly modulated presynaptically by GABA release from PG cells [54-57]. US-evoked bursts of activity in the PG cells would thus also reach the OSN terminals as a local inhibition, which we would not observe in the absence of an olfactory stimulus. This also suggests the future experiment of delivering a tailshock mid-odor presentation while imaging from the OSN terminals. Moreover, OSN synapses onto M/T cells have been previously reported to exhibit long-term potentiation [58] and long-term synaptic depression [59], though the potentially Hebbian nature of these synapses has never been tested.

If the OSNs do not respond to aversive stimulation directly, why is peripheral airflow both necessary for tailshock-evoked responses in the olfactory bulb and the basis for their timing? Even in the absence of explicit, experimenter-provided odorant, there is

a constant background of odorant in the room (plus the odor of the mouse itself and the experimenter himself) that could evoke a steady background of "spontaneous," respiration-locked peripheral input. Such activity has been reported before [60], and may be detectable in our data (analysis pending). If so, then the elimination of peripheral airflow would remove a normally-occurring tonic drive onto downstream neurons in the olfactory bulb that might drop them below threshold for response to a shock-evoked centrifugal input. This model is consistent with the observation that shock-evoked activity in the bulb only occurs during inhalations, suggesting that the bulbar neurons might be phasically shifting below and above threshold as a function of the respiratory cycle. Alternatively, one could think of this "spontaneous" peripheral input as a dynamic gate of the olfactory bulb circuitry. Taken at face value, this produces some strange but testable predictions, such as the idea that tailshocks presented during exhalation phase of the respiratory cycle might be less effective at inducing olfactory bulb plasticity or even at inducing odor-cued fear learning at all. Remarkably, this is consistent with a report from Iwabe et al., who found that in humans noxious electrical stimuli delivered to the hand during the inhalation phase of the respiratory cycle were systematically more painful, evoked larger N200 & P400 evoked potentials, evoked larger changes in skin conductance, and evoked larger changes in local blood-flow than the same stimuli delivered during the exhalation phase of the respiratory cycle in the same subjects [61]. It is also consistent with a recent finding (by a recent McGann Lab alum) that olfactory epithelial lesions disrupt respiratory-linked oscillations in the prefrontal cortex and in turn alter learned *auditory-cued* freezing [62].

References

1. Kass, M. D.; Pottackal, J.; Turkel, D. J.; McGann, J. P., Changes in the neural representation of odorants after olfactory deprivation in the adult mouse olfactory bulb. *Chem Senses* **2013,** *38* (1), 77-89.
2. Bliss, T. V.; Lomo, T., Long-lasting potentiation of synaptic transmission in the dentate area of the anaesthetized rabbit following stimulation of the perforant path. *J Physiol* **1973,** *232* (2), 331-56.
3. Clugnet, M. C.; LeDoux, J. E., Synaptic plasticity in fear conditioning circuits: induction of LTP in the lateral nucleus of the amygdala by stimulation of the medial geniculate body. *J Neurosci* **1990,** *10* (8), 2818-24.
4. Hebb, D. O., *The organization of behavior : a neuropsychological theory*. L. Erlbaum Associates: Mahwah, N.J., 2002.
5. Maren, S.; Aharonov, G.; Fanselow, M. S., Neurotoxic lesions of the dorsal hippocampus and Pavlovian fear conditioning in rats. *Behav Brain Res* **1997,** *88* (2), 261-74.
6. Maren, S.; Fanselow, M. S., Synaptic plasticity in the basolateral amygdala induced by hippocampal formation stimulation in vivo. *J Neurosci* **1995,** *15* (11), 7548-64.
7. Pavlov, I. P.; Anrep, G. V., *Conditioned reflexes; an investigation of the physiological activity of the cerebral cortex*. Oxford University Press: Humphrey Milford: London, 1927; p xv, 430 p.
8. Romanski, L. M.; LeDoux, J. E., Equipotentiality of thalamo-amygdala and thalamo-cortico-amygdala circuits in auditory fear conditioning. *J Neurosci* **1992,** *12* (11), 4501-9.
9. Ryan, T. J.; Roy, D. S.; Pignatelli, M.; Arons, A.; Tonegawa, S., Memory. Engram cells retain memory under retrograde amnesia. *Science* **2015,** *348* (6238), 1007-13.
10. Tonegawa, S.; Pignatelli, M.; Roy, D. S.; Ryan, T. J., Memory engram storage and retrieval. *Curr Opin Neurobiol* **2015,** *35*, 101-9.
11. Phillips, R. G.; LeDoux, J. E., Differential contribution of amygdala and hippocampus to cued and contextual fear conditioning. *Behav Neurosci* **1992,** *106* (2), 274-85.
12. Chen, C. F.; Barnes, D. C.; Wilson, D. A., Generalized vs. stimulus-specific learned fear differentially modifies stimulus encoding in primary sensory cortex of awake rats. *J Neurophysiol* **2011,** *106* (6), 3136-44.
13. Gdalyahu, A.; Tring, E.; Polack, P. O.; Gruver, R.; Golshani, P.; Fanselow, M. S.; Silva, A. J.; Trachtenberg, J. T., Associative fear learning enhances sparse network coding in primary sensory cortex. *Neuron* **2012,** *75* (1), 121-32.
14. Grossman, S. E.; Fontanini, A.; Wieskopf, J. S.; Katz, D. B., Learning-related plasticity of temporal coding in simultaneously recorded amygdala-cortical ensembles. *J Neurosci* **2008,** *28* (11), 2864-73.
15. Hager, A. M.; Dringenberg, H. C., Training-induced plasticity in the visual cortex of adult rats following visual discrimination learning. *Learn Mem* **2010,** *17* (8), 394-401.

16. Knight, D. C.; Smith, C. N.; Stein, E. A.; Helmstetter, F. J., Functional MRI of human Pavlovian fear conditioning: patterns of activation as a function of learning. *Neuroreport* **1999,** *10* (17), 3665-70.
17. Li, W.; Howard, J. D.; Parrish, T. B.; Gottfried, J. A., Aversive learning enhances perceptual and cortical discrimination of indiscriminable odor cues. *Science* **2008,** *319* (5871), 1842-5.
18. McGann, J. P., Associative learning and sensory neuroplasticity: how does it happen and what is it good for? *Learn Mem* **2015,** *22* (11), 567-76.
19. Morris, J. S.; Friston, K. J.; Dolan, R. J., Experience-dependent modulation of tonotopic neural responses in human auditory cortex. *Proc Biol Sci* **1998,** *265* (1397), 649-57.
20. Ohl, F. W.; Scheich, H., Learning-induced plasticity in animal and human auditory cortex. *Curr Opin Neurobiol* **2005,** *15* (4), 470-7.
21. Song, I.; Keil, A., Differential classical conditioning selectively heightens response gain of neural population activity in human visual cortex. *Psychophysiology* **2014,** *51* (11), 1185-94.
22. Weinberger, N. M., New perspectives on the auditory cortex: learning and memory. *Handb Clin Neurol* **2015,** *129*, 117-47.
23. Doucette, W.; Gire, D. H.; Whitesell, J.; Carmean, V.; Lucero, M. T.; Restrepo, D., Associative cortex features in the first olfactory brain relay station. *Neuron* **2011,** *69* (6), 1176-87.
24. Edeline, J. M.; Weinberger, N. M., Thalamic short-term plasticity in the auditory system: associative returning of receptive fields in the ventral medial geniculate body. *Behav Neurosci* **1991,** *105* (5), 618-39.
25. Edeline, J. M.; Weinberger, N. M., Subcortical adaptive filtering in the auditory system: associative receptive field plasticity in the dorsal medial geniculate body. *Behav Neurosci* **1991,** *105* (1), 154-75.
26. Edeline, J. M.; Weinberger, N. M., Associative retuning in the thalamic source of input to the amygdala and auditory cortex: receptive field plasticity in the medial division of the medial geniculate body. *Behav Neurosci* **1992,** *106* (1), 81-105.
27. Gao, E.; Suga, N., Experience-dependent plasticity in the auditory cortex and the inferior colliculus of bats: role of the corticofugal system. *Proc Natl Acad Sci U S A* **2000,** *97* (14), 8081-6.
28. Kass, M. D.; Rosenthal, M. C.; Pottackal, J.; McGann, J. P., Fear learning enhances neural responses to threat-predictive sensory stimuli. *Science* **2013,** *342* (6164), 1389-1392.
29. Jones, S. V.; Choi, D. C.; Davis, M.; Ressler, K. J., Learning-dependent structural plasticity in the adult olfactory pathway. *J Neurosci* **2008,** *28* (49), 13106-11.
30. Polley, D. B.; Read, H. L.; Storace, D. A.; Merzenich, M. M., Multiparametric auditory receptive field organization across five cortical fields in the albino rat. *J Neurophysiol* **2007,** *97* (5), 3621-38.
31. Berlau, K. M.; Weinberger, N. M., Learning strategy determines auditory cortical plasticity. *Neurobiol Learn Mem* **2008,** *89* (2), 153-66.
32. Kass, M. D.; Guang, S. A.; Moberly, A. H.; McGann, J. P., Changes in Olfactory Sensory Neuron Physiology and Olfactory Perceptual Learning After Odorant Exposure in Adult Mice. *Chem Senses* **2016,** *41* (2), 123-33.

33. Kass, M. D.; Czarnecki, L. A.; Moberly, A. H.; McGann, J. P., Differences in peripheral sensory input to the olfactory bulb between male and female mice. *Sci Rep* **2017,** *7*, 45851.
34. Fast, C. D.; McGann, J. P., Amygdalar Gating of Early Sensory Processing through Interactions with Locus Coeruleus. *J Neurosci* **2017,** *37* (11), 3085-3101.
35. Matsutani, S., Trajectory and terminal distribution of single centrifugal axons from olfactory cortical areas in the rat olfactory bulb. *Neuroscience* **2010,** *169* (1), 436-48.
36. Matsutani, S.; Yamamoto, N., Centrifugal innervation of the mammalian olfactory bulb. *Anat Sci Int* **2008,** *83* (4), 218-27.
37. Shepherd, G. M.; Greer, C. A.; Mazzarello, P.; Sassoe-Pognetto, M., The first images of nerve cells: Golgi on the olfactory bulb 1875. *Brain Res Rev* **2011,** *66* (1-2), 92-105.
38. Fletcher, M. L., Olfactory aversive conditioning alters olfactory bulb mitral/tufted cell glomerular odor responses. *Front Syst Neurosci* **2012,** *6*, 16.
39. Bozza, T.; McGann, J. P.; Mombaerts, P.; Wachowiak, M., In vivo imaging of neuronal activity by targeted expression of a genetically encoded probe in the mouse. *Neuron* **2004,** *42* (1), 9-21.
40. Mombaerts, P.; Wang, F.; Dulac, C.; Chao, S. K.; Nemes, A.; Mendelsohn, M.; Edmondson, J.; Axel, R., Visualizing an olfactory sensory map. *Cell* **1996,** *87* (4), 675-86.
41. Wachowiak, M.; Economo, M. N.; Diaz-Quesada, M.; Brunert, D.; Wesson, D. W.; White, J. A.; Rothermel, M., Optical dissection of odor information processing in vivo using GCaMPs expressed in specified cell types of the olfactory bulb. *J Neurosci* **2013,** *33* (12), 5285-300.
42. Kass, M. D.; McGann, J. P., Persistent, generalized hypersensitivity of olfactory bulb interneurons after olfactory fear generalization. *Neurobiol Learn Mem* **2017,** *146*, 47-57.
43. Kiyokage, E.; Pan, Y. Z.; Shao, Z.; Kobayashi, K.; Szabo, G.; Yanagawa, Y.; Obata, K.; Okano, H.; Toida, K.; Puche, A. C.; Shipley, M. T., Molecular identity of periglomerular and short axon cells. *J Neurosci* **2010,** *30* (3), 1185-96.
44. Backman, C. M.; Malik, N.; Zhang, Y.; Shan, L.; Grinberg, A.; Hoffer, B. J.; Westphal, H.; Tomac, A. C., Characterization of a mouse strain expressing Cre recombinase from the 3' untranslated region of the dopamine transporter locus. *Genesis* **2006,** *44* (8), 383-90.
45. Haddad, R.; Lanjuin, A.; Madisen, L.; Zeng, H.; Murthy, V. N.; Uchida, N., Olfactory cortical neurons read out a relative time code in the olfactory bulb. *Nat Neurosci* **2013,** *16* (7), 949-57.
46. Czarnecki, L. A.; Moberly, A. H.; Rubinstein, T.; Turkel, D. J.; Pottackal, J.; McGann, J. P., In vivo visualization of olfactory pathophysiology induced by intranasal cadmium instillation in mice. *Neurotoxicology* **2011,** *32* (4), 441-9.
47. Rothermel, M.; Wachowiak, M., Functional imaging of cortical feedback projections to the olfactory bulb. *Front Neural Circuits* **2014,** *8*, 73.
48. Markopoulos, F.; Rokni, D.; Gire, D. H.; Murthy, V. N., Functional properties of cortical feedback projections to the olfactory bulb. *Neuron* **2012,** *76* (6), 1175-88.

49. Kang, N.; Baum, M. J.; Cherry, J. A., Different profiles of main and accessory olfactory bulb mitral/tufted cell projections revealed in mice using an anterograde tracer and a whole-mount, flattened cortex preparation. *Chem Senses* **2011,** *36* (3), 251-60.
50. Adrian, E. D., Olfactory reactions in the brain of the hedgehog. *J Physiol* **1942,** *100* (4), 459-73.
51. Rogan, M. T.; Staubli, U. V.; LeDoux, J. E., Fear conditioning induces associative long-term potentiation in the amygdala. *Nature* **1997,** *390* (6660), 604-7.
52. Czarnecki, L. A.; Moberly, A. H.; Fast, C. D.; Turkel, D. J.; McGann, J. P., Multisensory expectations shape olfactory input to the brain. **2018**, 283242.
53. In 't Zandt, E. E.; Cansler, H. L.; Denson, H. B.; Wesson, D. W., Centrifugal Innervation of the Olfactory Bulb: A Reappraisal. *eNeuro* **2019,** *6* (1).
54. Aroniadou-Anderjaska, V.; Zhou, F. M.; Priest, C. A.; Ennis, M.; Shipley, M. T., Tonic and synaptically evoked presynaptic inhibition of sensory input to the rat olfactory bulb via GABA(B) heteroreceptors. *J Neurophysiol* **2000,** *84* (3), 1194-203.
55. McGann, J. P.; Pirez, N.; Gainey, M. A.; Muratore, C.; Elias, A. S.; Wachowiak, M., Odorant representations are modulated by intra- but not interglomerular presynaptic inhibition of olfactory sensory neurons. *Neuron* **2005,** *48* (6), 1039-53.
56. Murphy, G. J.; Darcy, D. P.; Isaacson, J. S., Intraglomerular inhibition: signaling mechanisms of an olfactory microcircuit. *Nat Neurosci* **2005,** *8* (3), 354-64.
57. Wachowiak, M.; McGann, J. P.; Heyward, P. M.; Shao, Z.; Puche, A. C.; Shipley, M. T., Inhibition [corrected] of olfactory receptor neuron input to olfactory bulb glomeruli mediated by suppression of presynaptic calcium influx. *J Neurophysiol* **2005,** *94* (4), 2700-12.
58. Ennis, M.; Linster, C.; Aroniadou-Anderjaska, V.; Ciombor, K.; Shipley, M. T., Glutamate and synaptic plasticity at mammalian primary olfactory synapses. *Ann N Y Acad Sci* **1998,** *855*, 457-66.
59. Mutoh, H.; Yuan, Q.; Knopfel, T., Long-term depression at olfactory nerve synapses. *J Neurosci* **2005,** *25* (17), 4252-9.
60. Verhagen, J. V.; Wesson, D. W.; Netoff, T. I.; White, J. A.; Wachowiak, M., Sniffing controls an adaptive filter of sensory input to the olfactory bulb. *Nat Neurosci* **2007,** *10* (5), 631-9.
61. Iwabe, T.; Ozaki, I.; Hashizume, A., The respiratory cycle modulates brain potentials, sympathetic activity, and subjective pain sensation induced by noxious stimulation. *Neurosci Res* **2014,** *84*, 47-59.
62. Moberly, A. H.; Schreck, M.; Bhattarai, J. P.; Zweifel, L. S.; Luo, W.; Ma, M., Olfactory inputs modulate respiration-related rhythmic activity in the prefrontal cortex and freezing behavior. *Nat Commun* **2018,** *9* (1), 1528.

Figure Captions

Figure 1. Tailshock evokes widespread activity in the olfactory bulb. A-D. Activity maps of the dorsal olfactory bulb of OSN-GCaMP(A), SA-GCaMP (B), PG-GCaMP(C), and M/T-GCaMP(D) mice averaged across several frames to highlight spatial activity pattern of the response to the presentation of Methyl Valerate (left) and A tail-shock (right) with corresponding fluorescence trace and respiration record for single trial (arrow is identifying region of interest used to extract trace).

Figure 2. Tail-shock-response amplitude distributions across cell types. A-D. Histogram depicting the distribution of the change in fluorescence of each region of interest in OSN-GCaMP(A), SA-GCaMP (B), PG-GCaMP(C), and M/T-GCaMP(D) mice.

Figure 3. Respiration coupled temporal evolution of shock response. Activity maps of the dorsal olfactory bulb of an OSN-GCaMP(A) and A SA-GCaMP (B) mouse during first and second inhalation after tail-shock with corresponding fluorescence traces and respiration records.

Figure 4. Tracheotomy eliminates tailshock-evoked activity in the olfactory bulb. The shock-evoked activity maps of the dorsal olfactory bulbs of OSN-GCaMP(A), PG-GCaMP(B), SA-GCaMP (C), and M/T-GCaMP(D) mice averaged across several frames to highlight spatial activity pattern of the response to presentation of Methyl Valerate (left), tail-shock (center) and tail-shock after tracheotomy(right).

Figure 5. Tracheotomy Prevents Aversive Activity in all Cell Populations Graph showing the average responses for each cell population during an odor trial, shock trial Before Tracheotomy, and A shock trial after tracheotomy

Figure 6. Unilateral naris occlusion prevents ipsilateral tailshock-evoked activity. Response maps from A SA-GCaMP (A.) and PG-GCaMP mouse to Methyl valerate (first column) and tail shock (second column). The first row is the baseline response. The second row is the response after the right naris is blocked. The bottom row shows the response map when the Left naris is blocked.

Figure 7. Various noxious stimuli evoke similar responses. A-D. Response map from single PG-GCaMP given Methyl valerate (A), Tail-shock (B), Thermal hindpaw stimulation (C), or CO2 (D).

Figures

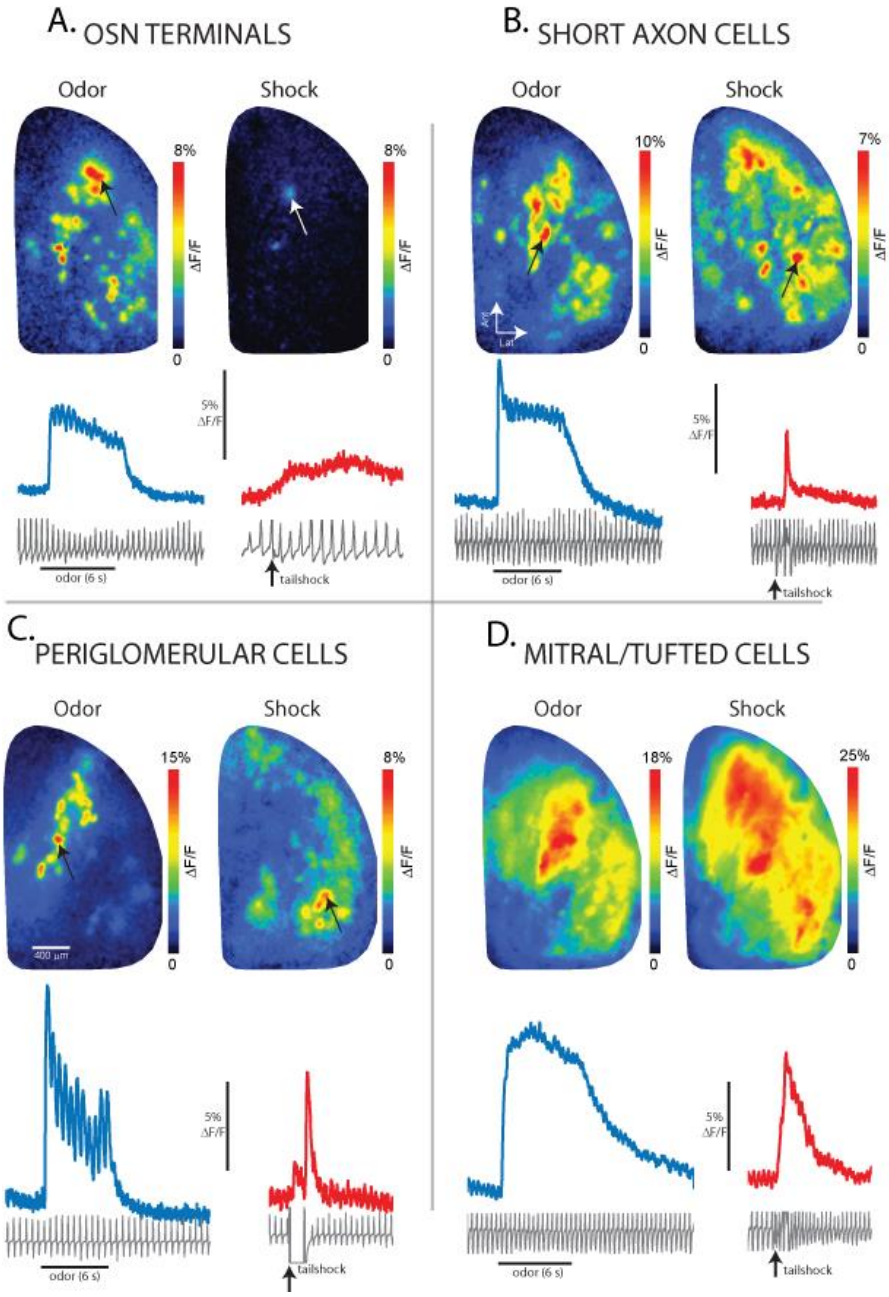

Figure 1. Tailshock Evoked Widespread Activity in the Olfactory Bulb

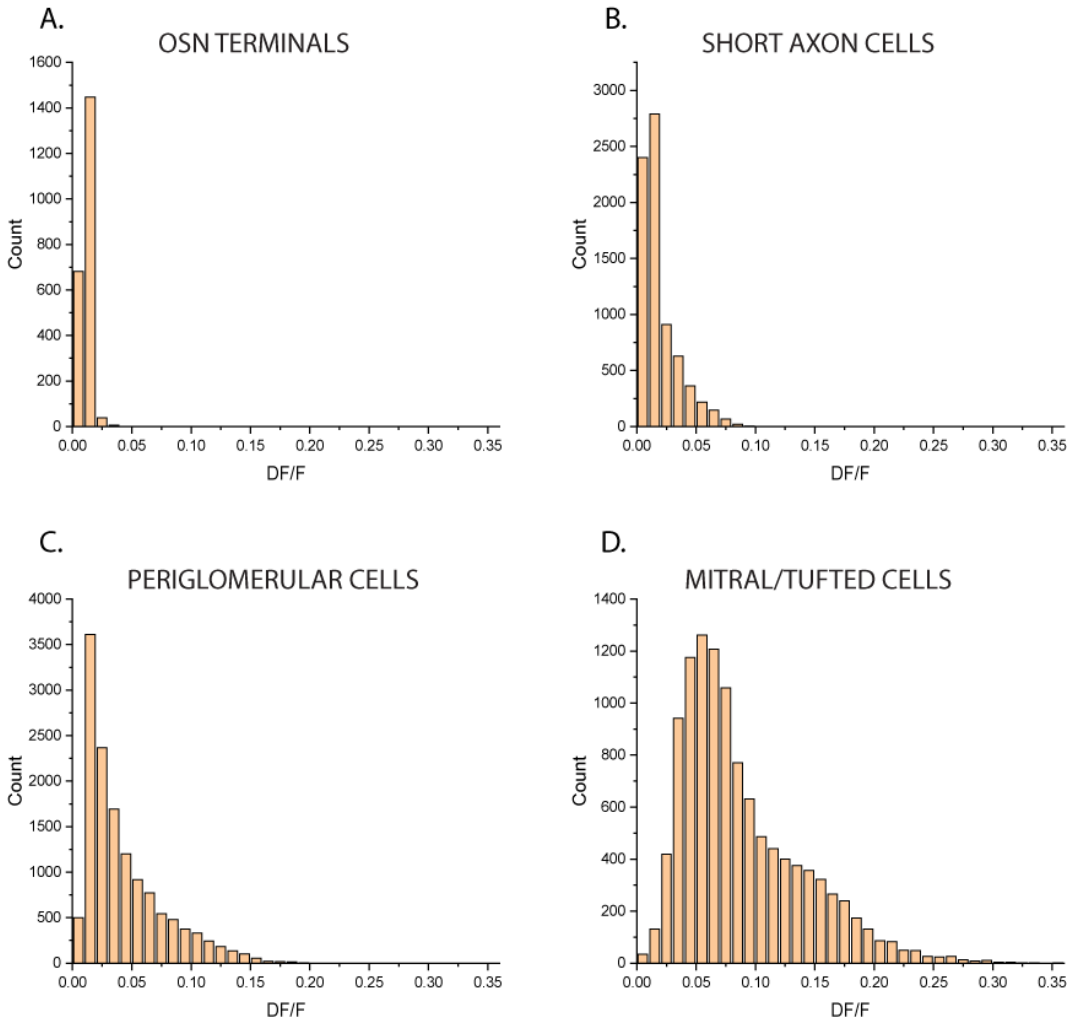

Figure 2. Tail-shock-Response Amplitude Distributions Across Cell Types

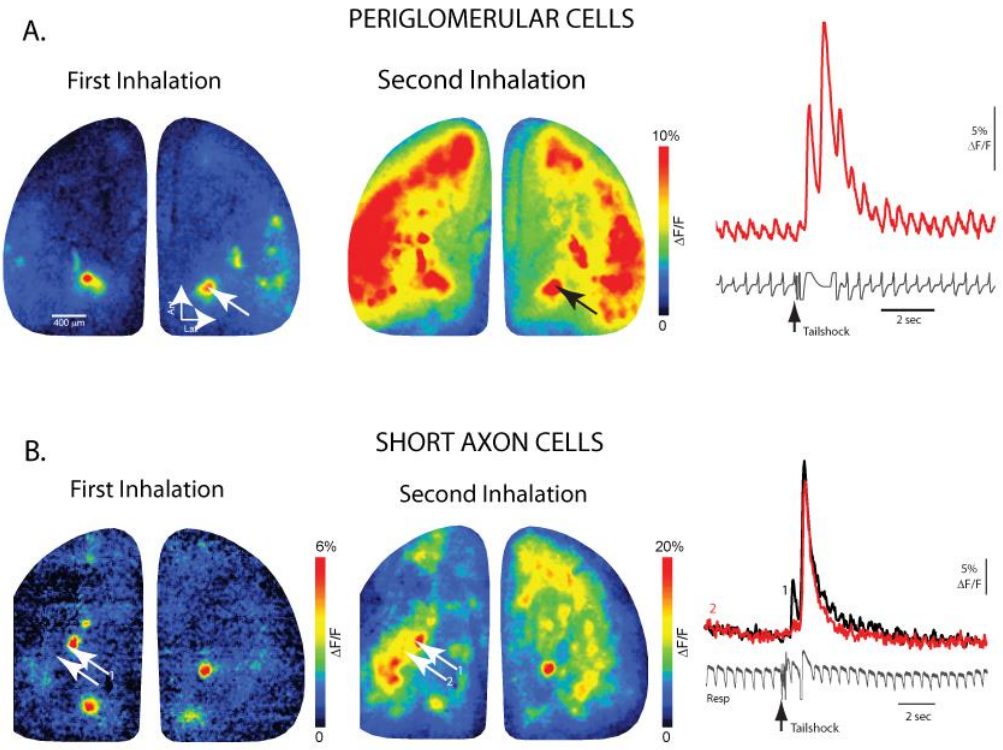

Figure 3. Respiration Coupled Temporal Evolution of Shock Response

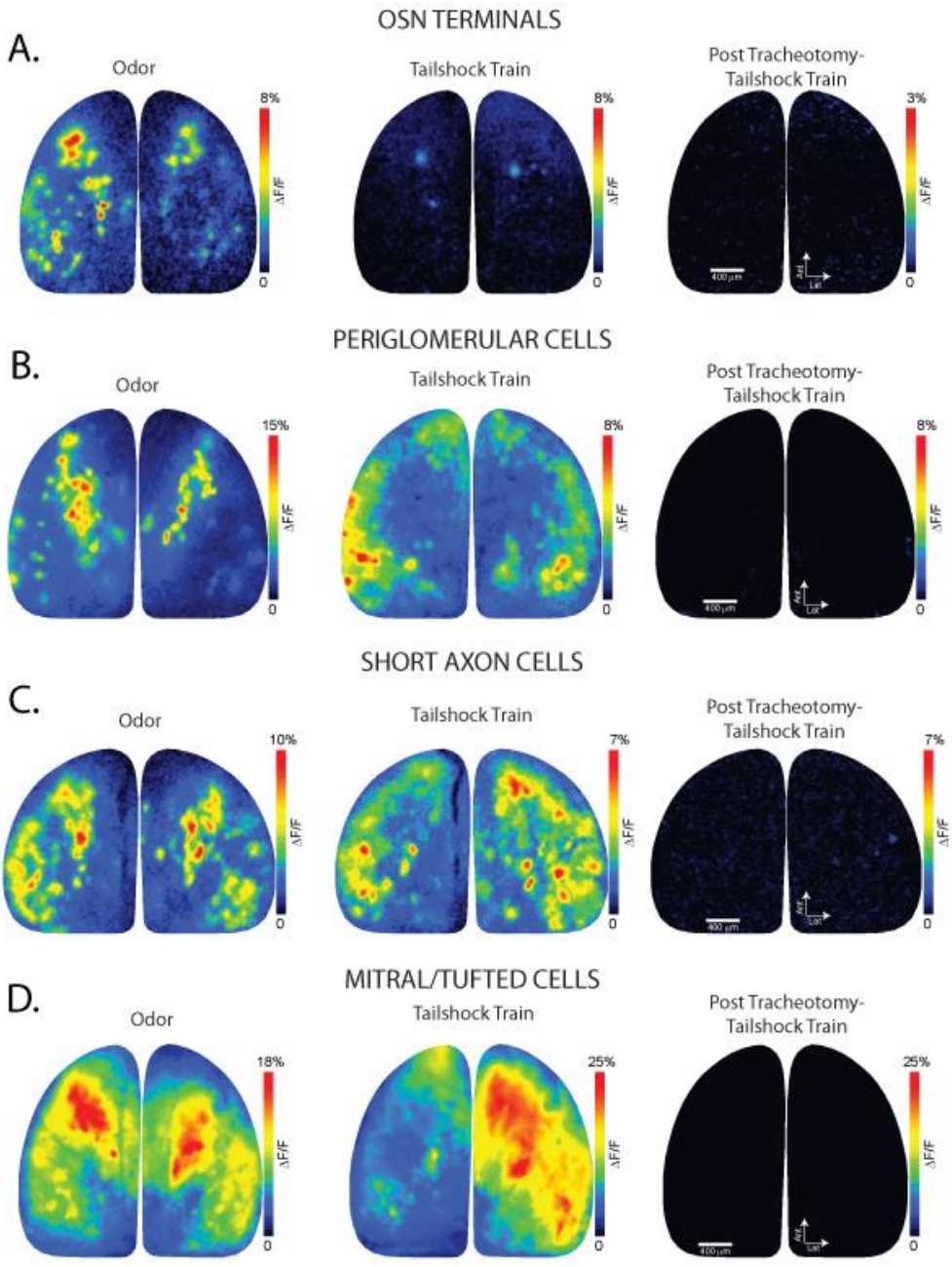

Figure 4. Tracheotomy Eliminates Tail-shock Evoked Activity in the Olfactory Bulb

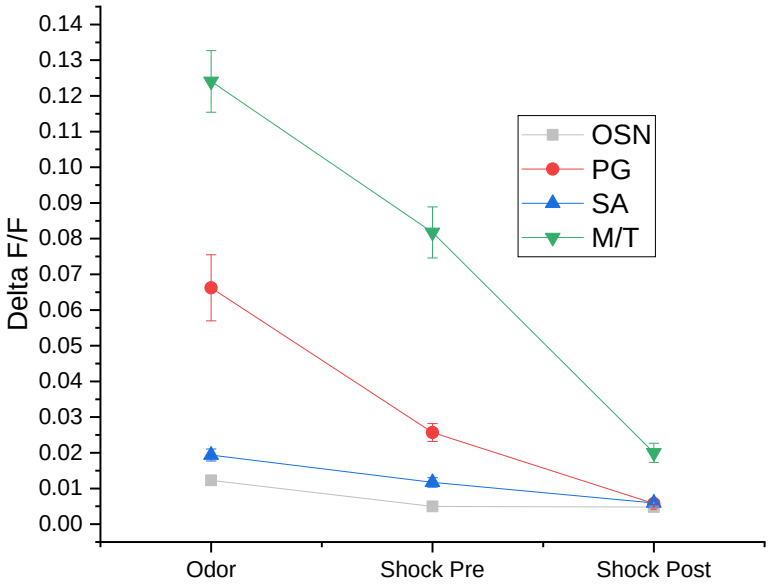

Figure 5. Tracheotomy Prevents Aversive Activity in all Cell Populations

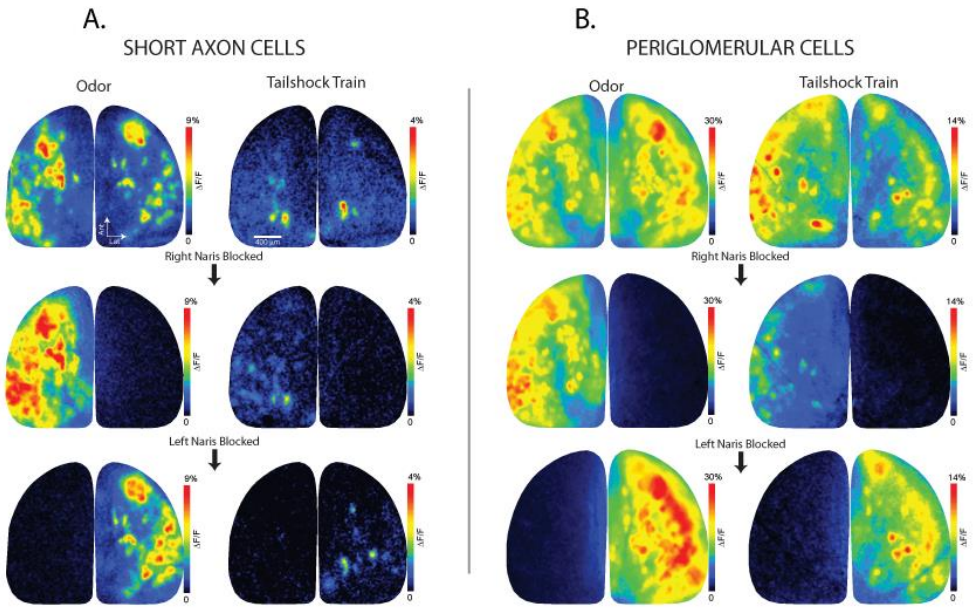

Figure 6. Unilateral Naris Occlusion Prevents Ipsilateral Tailshock-evoked Activity

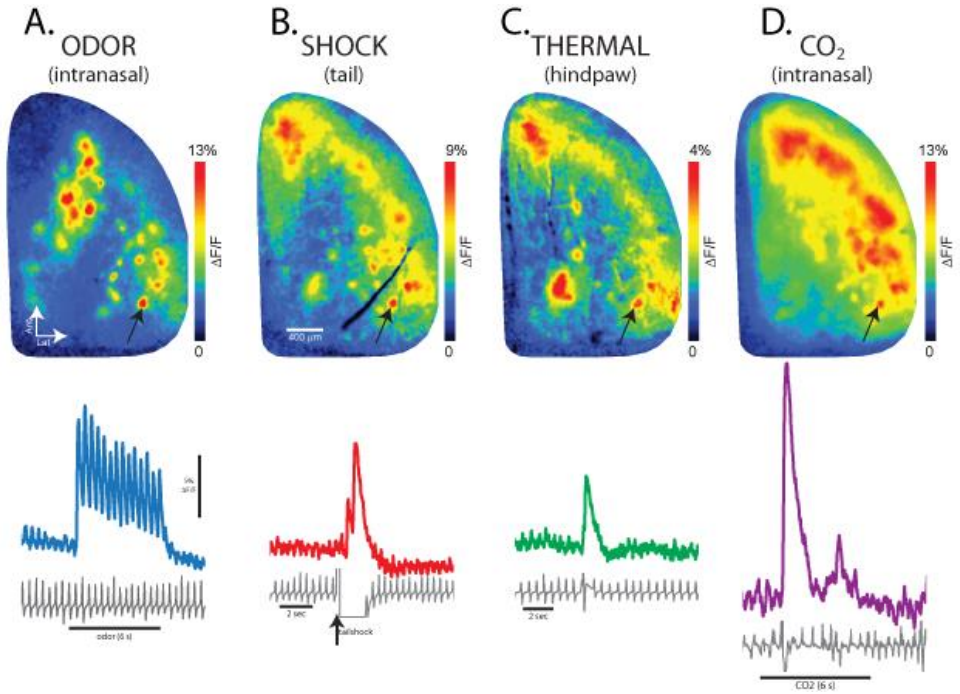

Figure 7. Various Noxious Stimuli Evoke Similar Responses